Volume Reduction of Traction Power Inverter EMI Filter Based on Mitigation Techniques at the Source

Volume Reduction of Traction Power Inverter EMI Filter Based on Mitigation Techniques at the Source

Markeljan Fishta
Dept. of Electronics and Telecom.
Politecnico di Torino
Torino, Italy
markeljan.fishta@polito.it

Franco Fiori
Dept. of Electronics and Telecom.
Politecnico di Torino
Torino, Italy
franco.fiori@polito.it

***Abstract*—Switching converters require effective EMI filters to comply with conducted emission regulations. However, these filters often pose significant challenges, being expensive, bulky and heavy. The situation is further exacerbated with the latest generation of converters, utilizing WBG semiconductor devices, which operate at higher switching frequencies. Reduction of the filter size can be achieved through conducted EMI mitigation techniques that address emissions at the source, particularly at low frequencies. This paper analyzes the CM filter volume reduction when using two CM mitigation techniques acting at the source, namely Spread Spectrum Modulation (SSM) and the Delay Compensation Technique (DCT). The considered techniques are implemented on a WBG traction power inverter and the volume reduction of the CM EMI filter is evaluated through computer simulations.**

***Index Terms*—EMI filtering, WBG, common mode, motor drives, frequency modulation, complex topology inverter**

I. Introduction

THE transition from traditional Silicon (Si) power devices to Wide Band Gap (WBG) ones is revolutionizing power electronics, particularly in the automotive sector, enabling enhanced efficiency and power density [1]. Despite these advantages, this transition poses significant challenges in the design of the Electromagnetic Interference (EMI) filters, necessary to comply with conducted emissions limits [2]. With WBG transistors, there has been a remarkable increase in switching frequency and commutation speed, with WBG-based inverters reported to operate up to the MHz range [3]. Automotive systems, including onboard converters and charger blocks, have seen similar frequency increases. Conversely, motor drive blocks, like the inverter shown in Fig. 1, have maintained stable frequencies around 10 kHz to 20 kHz, leveraging the reduced losses of WBG devices to enhance power density [1]. However, guidelines from the U.S. Department of Energy (DoE) for the years 2020 to 2025, target switching frequencies in traction inverters within the range of 30 kHz to 50 kHz [4], meaning that the switching frequency is set to increase. Consequently, the required insertion loss of EMI filters escalates due to the shifting of the most energetic switching harmonics within the regulated frequency range, starting from 150 kHz [2]. The increase in insertion loss directly translates into higher costs and larger physical dimensions for the filter, potentially occupying up to one fifth of the entire inverter volume [5].

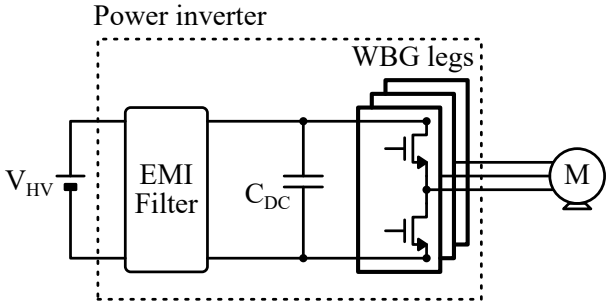

Fig. 1. Three phase WBG motor drive system.

To address these challenges, recent efforts have focused on EMI filter design methods to reduce volume [6]. An effective approach involves adopting techniques that mitigate EMI at the source, thereby relaxing the requirements on passive filters. A comprehensive overview of mitigation techniques at the source for conducted EMI is given in [7], according to which low-frequency (LF) EMI spectral components are primarily influenced by PWM sequences, whereas high-frequency (HF) components are mainly determined by switching transients. Consequently, since the passive filter design is heavily influenced by the LF switching harmonics [8], techniques such as variable switching frequency and complex inverter topology prove valuable for reducing filter volume, whereas methods focused on controlling switching transients are effective at higher frequencies [9].

This paper provides a comparison between the Spread Spectrum Modulation (SSM) and Delay Compensation Techniques (DCT), focusing on the volume reduction of the CM passive EMI filter. The paper structure is organized as follows: in Sect. II the spread spectrum and the auxiliary leg techniques are reviewed, with particular attention to their effectiveness at LF. Sect. III presents the CM passive EMI filter design and the volume comparison between the different solutions. Sect. IV concludes the paper.

II. CM disturbance mitigation at the source

To analyze the effectiveness of the two mitigation techniques, one of the inverter legs is considered. Referring to the main leg shown in Fig. 2, the circuit comprises of two

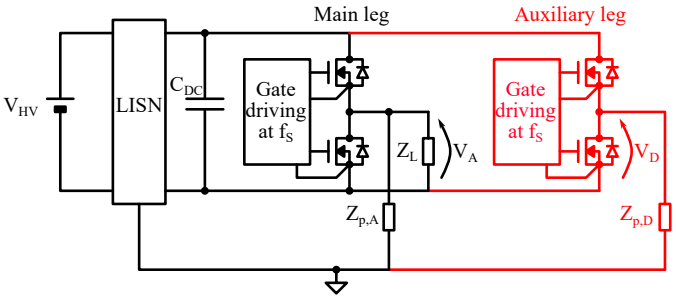

Fig. 2. Simplified circuit for the evaluation of the CM output voltage. The black portion of the circuit is the main switching leg driving the load while the red portion is the auxiliary leg, which is used to cancel the CM output voltage in the modified topology inverter.

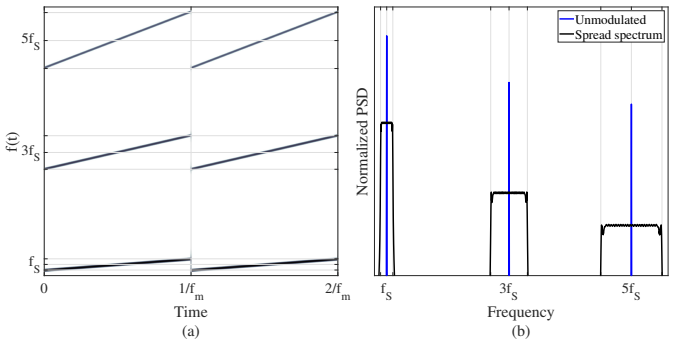

Fig. 3. Illustration of the triangular frequency modulation of a PWM signal: (a) time-frequency diagram highlighting the modulation frequency and (b) normalized PSD illustrating the energy spread for the first three harmonics.

equal power transistors driven at frequency f_{S}, driving the load impedance Z_{L}. The conducted CM disturbance is observed at the LISNs [2]. This voltage arises from the CM voltage at the output of the switching circuit, propagating to the LISNs due to the parasitic impedance $Z_{\mathrm{p,A}}$, modeling the capacitive coupling of the power devices to the heatsink. Therefore, analyzing the CM voltage at the output provides insight into the CM voltage conducted to the LISNs [10].

The phase voltage v_{A} can be approximated by a trapezoidal signal with frequency f_{S}, amplitude A, duty cycle D and transition time t_{t}. Hence, a switching leg acts as EMI source having large amounts of energy near the switching frequency f_{S} and its harmonics. The presence of these peaks in the spectrum of the signal can lead to not comply with conducted emission limits [2]. In the following, two techniques reducing the harmonics at the source will be briefly presented.

A. Spread Spectrum Modulation of PWM signal

The SSM is a technique to mitigate electromagnetic interference at the source, by introducing a variation in the instantaneous switching frequency $\hat{f}_{\mathrm{S}}(t)$, following a specific modulation profile. When the frequency of the PWM switching voltage is modulated, the energy of each harmonic is spread over Carson's bandwidth [11]. Frequency modulation results in an instantaneous frequency for the k^{th} harmonic given by

$$\hat{f}_{\mathrm{k}}(t) = f_{\mathrm{k0}}\left[1 + \frac{k\Delta f}{f_{\mathrm{k0}}} m(t)\right] \tag{1}$$

where Δf is the frequency deviation, f_{k0} is the central frequency of the k^{th} harmonic, $m(t) \in [-1, 1]$ is the modulation profile and its frequency f_{m} is called modulation frequency. The modulation index for each harmonic is given by

$$m_{\mathrm{k}} = \frac{k\Delta f}{f_{\mathrm{m}}}. \tag{2}$$

A time-frequency diagram, as shown in Fig. 3(a), illustrates the scaling of the frequency deviation with the order of the harmonics while simultaneously displaying the frequency modulation profile. In Fig. 3(b), the power spreading of the single harmonics can be observed. It is worth noting that if the frequency deviation is too large, the spreading bands of two harmonics can overlap, diminishing the effectiveness of the spreading [12]. The parameters of the spreading play a crucial role in the efficacy of the technique for EMI reduction. Generally, as Δf increases, the EMI peak decreases. For a certain Δf, there exists an optimum modulation index that guarantees the largest EMI reduction [13].

B. Delay Compensation Technique

The addition of an auxiliary leg to a three-phase inverter was introduced in [14] as a solution to reduce the CM voltage at the output of the inverter. Recently, such technique has been combined with the DCT, leading to significant enhancements aimed to achieve superior CM conducted EMI reduction [15]–[17]. By introducing a dummy leg and suitably selecting the commands of the additional leg transistors, the common-mode voltage at the output can theoretically be zeroed. In practice the cancellation cannot be perfect due to misalignment of the output phase voltages [15]–[17]. To illustrate the effect of the auxiliary leg, the circuit in Fig. 2 is considered. The circuit consists of the main leg A and the auxiliary leg D, which is switched in a complementary way with respect to A. Assuming that the voltage v_{D} is complementary to v_{A} except for a delay t_{d}, the CM output voltage $v_{\mathrm{AV}} = \frac{v_{\mathrm{A}}+v_{\mathrm{D}}}{2}$ consists of pulses in correspondence of the switching instants. The time-domain and the frequency-domain representation of such voltage are depicted in Fig. 4. As can be seen from the time-domain, the common mode voltage is constant, except near the commutation instants, owing to the misalignment of the two voltages. This leads to a reduced amplitude of the peaks in the frequency domain, as shown in the right plot.

III. Filter Design and Comparison

The EMI filter design considers a three-phase traction power inverter, as the one in Fig. 1. The specifications of the inverter are provided in Table I. In accordance with the DoE recommendations for the next years [4], the switching frequency has been set at 50 kHz. The reference case is the Space Vector PWM (SVPWM) switching inverter. Subsequently, two EMI mitigation techniques were applied to the same inverter: SSM and DCT, respectively. Concerning the auxiliary leg, it was loaded with a capacitance equal to the CM capacitance of

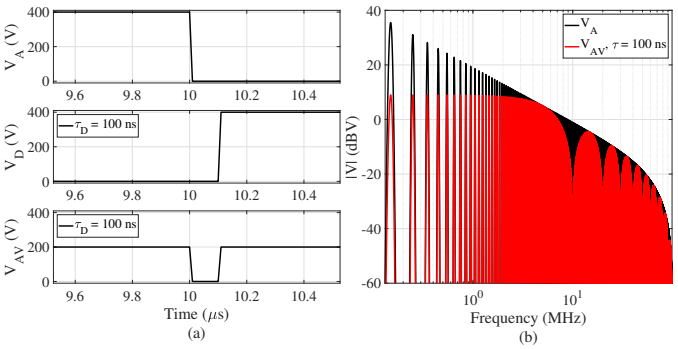

Fig. 4. Illustration of the CM output voltage (a) in the time domain and (b) in the frequency domain, for the single-leg and after the addition of the auxiliary leg.

TABLE I
INVERTER SPECIFICATIONS.

Parameter	Value	Unit
V_{HV}	400	V
f_{S}	50	kHz
C_{DC}	80	μF
I_{DC}	100	A

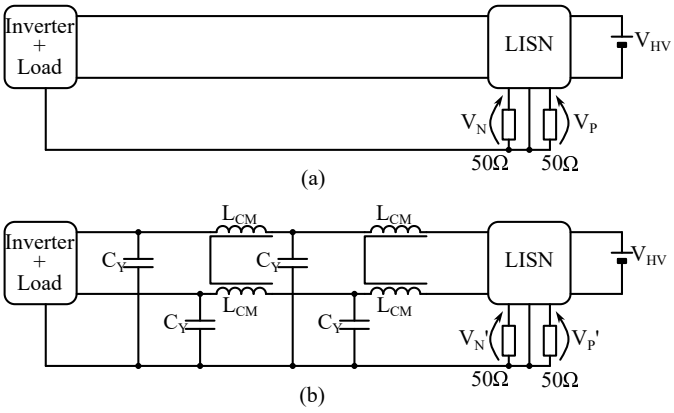

Fig. 5. Inverter simulation testbench (a) without EMI filter and (b) with EMI filter.

one motor phase. Regarding the spread spectrum, assuming a 10 % relative frequency deviation, a maximum deviation of $\Delta f = 5\,\mathrm{kHz}$ results at the fundamental frequency. The spreading has been optimized at the third harmonic $f_{30} = 150\,\mathrm{kHz}$, with frequency deviation $3\Delta f = 15\,\mathrm{kHz}$ and an optimal modulation index $m_{\mathrm{opt}} = 1.5$. This choice results in a modulation frequency of $f_{\mathrm{m,opt}} = 10\,\mathrm{kHz}$. In order to perform the CM EMI filter design, the conducted CM disturbance was extracted from simulation using the test bench in Fig. 5 (a). The CM voltage at the LISNs is evaluated as

$$v_{\mathrm{CM}} = \frac{v_{\mathrm{P}} + v_{\mathrm{N}}}{2}. \tag{3}$$

The resulting voltage is analyzed using an EMI receiver emulator [18], yielding the CM disturbance in the frequency domain, denoted as V_{CM}, as represented in Fig. 6. From the plot it results that the SVPWM modulated inverter exhibits the

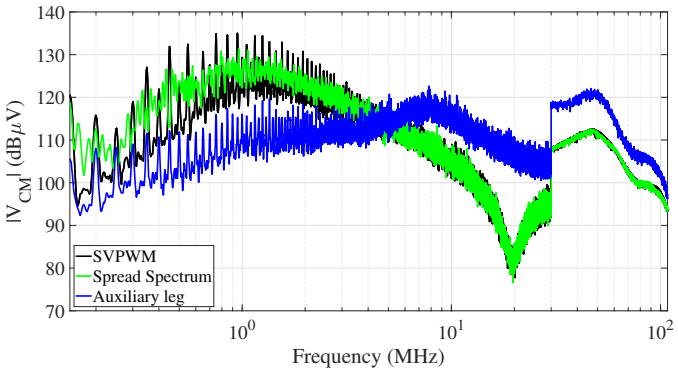

Fig. 6. CM emission spectra of the three different configurations considered, from circuit simulation, at the LISNs.

TABLE II
FILTER PARAMETERS COMPARISON.

Parameter	SVPWM	Spread spectrum	Aux leg
C_{Y}	100 nF	100 nF	100 nF
L_{CM}	130 μH	100 μH	40 μH
Material	Nanocrystalline	Nanocrystalline	Nanocrystalline

highest CM conducted emissions at low frequency. Applying spread spectrum with optimization at 150 kHz provides a few dB reduction of the third harmonic, which is in good agreement with theoretical expected reduction for the selected frequency deviation [13]. The addition of the dummy leg, on the other hand, achieves a more substantial reduction of around 15 dB at the same frequency, while giving rise to an increase of EMI at higher frequencies. Subsequently, CM EMI filter design was undertaken following a standard procedure outlined in [8]. Additionally, HF effects like the magnetic permeability variation [19] and capacitor parasitics were considered in the insertion loss (IL) simulations, performed using the testbench depicted in Fig. 5, where C_{Y} and L_{CM} are the CM capacitance and inductance, respectively. The employed filter topology was a two-stage CL configuration, and the resulting values for the different designs are summarized in Table II. The IL was evaluated as

$$IL = 20\log\left(\frac{V_{\mathrm{CM}}}{V'_{\mathrm{CM}}}\right) \tag{4}$$

and the comparison between the achieved IL and the required one for each case is shown in Fig. 7. As observed, the CM filter achieves the desired attenuation in all cases. However, from Table II it results that, with equal CM capacitance, the required CM inductance decreases when employing CM reduction techniques at the source. The volume of the CM choke was estimated following the method proposed in [20]

$$V_{\mathrm{L}} = k_{\mathrm{L0}} L_{CM} + k_{\mathrm{L1}} I_{\mathrm{DC}} + k_{\mathrm{L2}} L_{CM} I_{\mathrm{DC}}^2 + k_{\mathrm{L3}} \tag{5}$$

where I_{DC} is the DC current going through the choke, and k_{Li} are coefficients [20]. The key finding is that employing optimally designed spread spectrum results in a 21% reduction in the volume of the CM choke, while adding a dummy leg to the inverter achieves a substantial 63% reduction. The

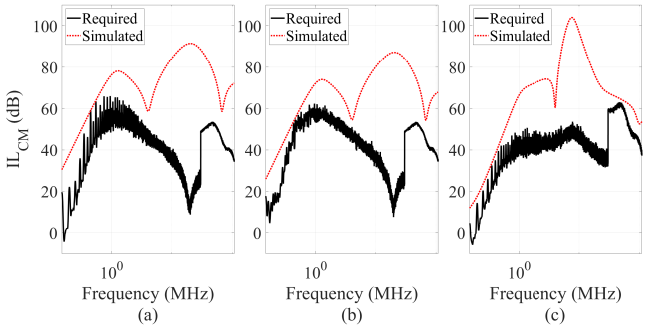

Fig. 7. Filter insertion loss simulation for (a) SVPWM inverter, (b) spread-spectrum inverter and (c) auxiliary leg inverter. For each plot the continuous trace represents the required IL, the dashed trace is the analytical IL for nominal filter and the dotted trace is the simulated IL for CM filter including magnetic losses and CY parasitics.

observed HF EMI increase in the dummy leg case does not impact the filter volume in a significant way, since the volume is related to the LF IL and smaller passive components can be used to control the HF emissions. No active control of the τ_{D} parameter was implemented in the simulations, meaning that its value varied with load current in the range $(7\,\mathrm{ns}, 30\,\mathrm{ns})$. Further enhancements could be achieved with the adoption of techniques for finely controlling the alignment of the output voltages, as proposed in [15]–[17].

IV. Conclusions

This paper investigated the volume reduction of the CM passive filter in a WBG traction power inverter. The considered conducted CM EMI reduction techniques at the source included spread spectrum and the addition of an auxiliary leg to the inverter. Simulation results of the conducted emissions revealed that spread spectrum optimization near the lower frequency limit of the regulations, i.e. $150\,\mathrm{kHz}$, provides a modest attenuation of the EMI peak at that frequency. In contrast, the addition of a dummy leg to the inverter demonstrated a significant $15\,\mathrm{dB}$ peak reduction at the same frequency.
For the considered case studies, three CM passive filters were designed. It was observed that the required CM inductance decreases slightly when implementing spread spectrum, while it experiences a drastic reduction when employing the auxiliary leg technique. The evaluation, using a volumetric model, indicated a 21% reduction in CM inductor volume when using spread spectrum modulation. Adding the dummy leg to the inverter, despite the increase of the HF EMI, led to a 63% reduction in the filter volume.

References

[1] T. Van Do, J. P. F. Trovão, K. Li, and L. Boulon, "Wide-Bandgap Power Semiconductors for Electric Vehicle Systems: Challenges and Trends," IEEE Vehicular Technology Magazine, vol. 16, no. 4, pp. 89–98, Dec. 2021, doi: 10.1109/MVT.2021.3112943.

[2] "CISPR 25:2021 - Vehicles, boats and internal combustion engines - Radio disturbance characteristics - Limits and methods of measurement for the protection of on-board receivers." Dec. 2021. Accessed: Oct. 04, 2023. [Online]. Available: https://webstore.iec.ch/publication/64645

[3] C.-T. Ma and Z.-H. Gu, "Review of GaN HEMT Applications in Power Converters over 500 W," Electronics, vol. 8, no. 12, Art. no. 12, Dec. 2019, doi: 10.3390/electronics8121401.

[4] C. S. Goli, S. Essakiappan, P. Sahu, M. Manjrekar, and N. Shah, "Review of Recent Trends in Design of Traction Inverters for Electric Vehicle Applications," in 2021 IEEE 12th International Symposium on Power Electronics for Distributed Generation Systems (PEDG), Jun. 2021, pp. 1–6. doi: 10.1109/PEDG51384.2021.9494164.

[5] D. O. Boillat, F. Krismer, and J. W. Kolar, "EMI Filter Volume Minimization of a Three-Phase, Three-Level T-Type PWM Converter System," IEEE Transactions on Power Electronics, vol. 32, no. 4, pp. 2473–2480, Apr. 2017, doi: 10.1109/TPEL.2016.2617085.

[6] L. Zhai, G. Hu, C. Song, M. Lv, and X. Zhang, "Comparison of Two Filter Design Methods for Conducted EMI Suppression of PMSM Drive System for Electric Vehicle," IEEE Transactions on Vehicular Technology, vol. 70, no. 7, pp. 6472–6484, Jul. 2021, doi: 10.1109/TVT.2021.3080924.

[7] Z. Zhang, Y. Hu, X. Chen, G. W. Jewell, and H. Li, "A Review on Conductive Common-Mode EMI Suppression Methods in Inverter Fed Motor Drives," IEEE Access, vol. 9, pp. 18345–18360, 2021, doi: 10.1109/ACCESS.2021.3054514.

[8] H. Movagharnejad and A. Mertens, "Design Methodology for Dimensioning EMI Filters for Traction Drives with SiC Inverters," in 2021 23rd European Conference on Power Electronics and Applications (EPE'21 ECCE Europe), Ghent, Belgium: IEEE, Sep. 2021, pp. 1–10. doi: 10.23919/EPE21ECCEEurope50061.2021.9570678.

[9] E. Raviola and F. Fiori, "An Adaptive Method to Reduce Undershoots and Overshoots in Power Switching Transistors Through a Low-Complexity Active Gate Driver," IEEE Transactions on Power Electronics, vol. 38, no. 3, pp. 3235–3245, Mar. 2023, doi: 10.1109/TPEL.2022.3221187.

[10] M. Antivachis, P. S. Niklaus, D. Bortis, and J. W. Kolar, "Input/output EMI filter design for three-phase ultra-high speed motor drive gan inverter stage," CPSS Transactions on Power Electronics and Applications, vol. 6, no. 1, pp. 74–92, Mar. 2021, doi: 10.24295/CPSSTPEA.2021.00007.

[11] H. S. Black, Modulation Theory. Van Nostrand, 1953.

[12] D. Gonzalez et al., "Conducted EMI Reduction in Power Converters by Means of Periodic Switching Frequency Modulation," IEEE Transactions on Power Electronics, vol. 22, no. 6, pp. 2271–2281, Nov. 2007, doi: 10.1109/TPEL.2007.909257.

[13] F. Pareschi, R. Rovatti, and G. Setti, "EMI Reduction via Spread Spectrum in DC/DC Converters: State of the Art, Optimization, and Tradeoffs," IEEE Access, vol. 3, pp. 2857–2874, 2015, doi: 10.1109/ACCESS.2015.2512383.

[14] A. L. Julian, G. Oriti, and T. A. Lipo, "Elimination of common-mode voltage in three-phase sinusoidal power converters," IEEE Transactions on Power Electronics, vol. 14, no. 5, pp. 982–989, Sep. 1999, doi: 10.1109/63.788504.

[15] E. Raviola, M. Roman, L. Zai, and F. Fiori, "Reduction of CM Conducted Emission With a Small Dummy Leg and the Delay Compensation Technique," in 2023 IEEE Symposium on Electromagnetic Compatibility & Signal/Power Integrity (EMC+SIPI), Jul. 2023, pp. 542–547. doi: 10.1109/EMCSIPI50001.2023.10241590.

[16] M. Perotti and F. Fiori, "Investigating the EMI Mitigation in Power Inverters Using Delay Compensation," IEEE Trans. Power Electron., vol. 34, no. 5, pp. 4270–4278, May 2019, doi: 10.1109/TPEL.2018.2858015.

[17] M. Perotti and F. Fiori, "A Closed Loop Delay Compensation Technique to Mitigate the Common Mode Conducted Emissions of Bipolar PWM Switched Circuits," IEEE Trans. Power Electron., vol. 36, no. 5, pp. 5450–5459, May 2021, doi: 10.1109/TPEL.2020.3031349.

[18] A. Bendicks, T. Dörlemann, C. Krause, and S. Frei, "MATLAB/Octave function to evaluate time-domain signals according to the measurement bandwidth and average/peak detector of EMI test receivers," pp. 459–466, 2022, doi: 10.15488/12605.

[19] K. Nomura, N. Kikuchi, Y. Watanabe, S. Inoue, and Y. Hattori, "Novel SPICE model for common mode choke including complex permeability," in 2016 IEEE Applied Power Electronics Conference and Exposition (APEC), Mar. 2016, pp. 3146–3152. doi: 10.1109/APEC.2016.7468314.

[20] S. Dey and A. Mallik, "A Comprehensive Review of EMI Filter Network Architectures: Synthesis, Optimization and Comparison," Electronics, vol. 10, no. 16, Art. no. 16, Jan. 2021, doi: 10.3390/electronics10161919.